

Formation of Cu_3BiS_3 thin films via sulfurization of Bi-Cu metal precursors

D. Colombara^a, L. M. Peter^a, K. Hutchings^b, K. D. Rogers^b, S. Schäfer^c, J. T. R. Dufton^a and M. S. Islam^a

^aDepartment of Chemistry, University of Bath, Bath BA27AY, UK

^bCentre for Materials Science and Engineering, Cranfield University, Shrivenham, SN68LA, UK

^cEnthone GmbH Elisabeth-Selbert-Strasse 4, Langenfeld 40764, Germany

Abstract

Thin films of Cu_3BiS_3 have been produced by conversion of stacked and co-electroplated Bi-Cu metal precursors in the presence of elemental sulfur vapour. The roles of sulfurization temperature and heating rate in achieving single-phase good quality layers have been explored. The potential loss of Bi during the treatments has been investigated, and no appreciable compositional difference was found between films sulfurized at 550 °C for up to 16 hours. The structural, morphological and photoelectrochemical properties of the layers were investigated in order to evaluate the potentials of the compound for application in thin film photovoltaics.

Keywords:

Wittichenite, Availability, Electrodeposition, Sulfurization, RTP, Photoelectrochemistry, Solar cell.

1. Introduction

The search for earth-abundant non-toxic materials for large scale deployment of photovoltaics is becoming increasingly important. Current technologies using rare elements such as indium and gallium are unlikely to be able to satisfy the rapidly growing demand for thin film solar cells. The United States Geological Survey assessed the 2010 annual world mine production of Bi as 7600 t with estimated world reserves of 320000 t. These figures can be compared with the annual world production (only by refinery) of 574 t for In with no established estimation for its world reserves [1]. During 2010, the price for Bi was below 20 U.S. \$ kg^{-1} , while In had an average price over 500 U.S. \$ kg^{-1} . Owing to its low toxicity as well as relatively low cost, Bi has been considered in the framework of the COST Action 531 as a potential candidate for the development of lead-free soldering alloys [2-5], and some of its compounds are employed in a range of pharmaceutical and cosmetic products.

The potential application of the sulfosalt Cu_3BiS_3 as a *p*-type absorber film in photovoltaics was first considered by Nair et al. [6]. This compound, which occurs naturally as the mineral *Wittichenite*, crystallises in an orthorhombic unit cell ($a = 7.723 \text{ \AA}$, $b = 10.395 \text{ \AA}$, $c = 6.715 \text{ \AA}$) [7] containing 4 formula units. Its low temperature polymorph belongs to the space group $\text{P}2_12_12_1$, so that its structure differs from that of the cubic and tetragonal semiconductors derived from the Si crystal structure, which form the basis of current solar cell technology. The coordination of

1 the Cu atoms is nearly trigonal planar (Fig. 1), while the Bi atoms show a particularly
2 unusual trigonal pyramidal geometry with the three nearest sulfur atoms (Fig. 2). The
3 structure is comprised of infinite chains of edge-sharing distorted square pyramidal
4 BiS_5 units aligned along the a axis, separated by the CuS_3 units (Fig. 3).

5 Makovicky et al. [8] have found that Cu_3BiS_3 undergoes a series of phase
6 transitions, starting from 118.5°C , that involve reorganization of the Cu distribution
7 with their conversion from a stationary to a mobile state, turning the compound into a
8 solid electrolyte at relatively low temperatures. The recent results of Mesa et al. [9]
9 show that the optical and electrical properties of Cu_3BiS_3 , including a direct forbidden
10 band gap of 1.4 eV [10], confirm its potential for application as a solar absorber in
11 single heterojunction thin film solar cells.

12 Thin films of crystallographically pure Cu_3BiS_3 have been synthesized by
13 annealing diffusion couples of chemical bath deposited Bi_2S_3 and CuS layers [6] as
14 well as chemical bath deposited CuS and thermally evaporated Bi layers [11].
15 However, it is unclear from these reports whether such methods lead to films with
16 suitable morphology for the application in solar cells (Scanning Electron Microscopy
17 -SEM- images were not published). By contrast, a one-step reactive sputter deposition
18 route developed by Gerein et al. [10] produces phase pure Cu_3BiS_3 films with optical,
19 electrical and morphological properties that are ideal for incorporation into devices. A
20 combinatorial strategy for rapid device screening was reported to be in progress [12,
21 13], but no results have yet been published. Previous work by the same group [14] on
22 a two-step synthesis process using metal and metal sulfide precursors demonstrated
23 complete conversion into the phase pure ternary chalcogenide under H_2S , but the
24 morphology of the films was found to be unsuitable for use in photovoltaics. Best
25 results were achieved with co-sputtered precursors at processing temperatures as low
26 as 270°C , but with very long heating times (> 16 h). According to this report, the
27 useful range of processing conditions for the formation of the ternary chalcogenide is
28 limited by the volatility of Bi above 300°C , since treatments at higher temperatures
29 resulted in Bi depletion [14].

30 Co-electrodeposition of metal precursors followed by conversion into the
31 chalcogenide has proved to give promising results on laboratory scale $\text{Cu}_2\text{ZnSnS}_4$
32 (CZTS) -based devices [15]. The method has potential for fabrication of large area
33 uniform films with low cost capital equipment. The present study sets out to
34 investigate the conversion of electroplated layered Cu/Bi/Cu precursors and
35 homogenous Cu-Bi deposits of appropriate overall composition into Cu_3BiS_3 films
36 with a continuous morphology. Sulfur incorporation was achieved by the action of the
37 chalcogen vapour on the metal precursors. Following the approach taken previously in
38 a study of the $\text{CuSb}(\text{S},\text{Se})_2$ system, the conversion of the single elements to binary
39 sulfides was investigated as well as the subsequent reaction to form the ternary
40 chalcogenide[16].

41 42 43 **2. Experimental**

44 45 *2.1 Precursor preparation and sulfurization*

46
47 Sequential electrodeposition of Cu/Bi/Cu layers with the desired elemental ratio was
48 carried out by Enthone GmbH R&D laboratories using commercially available
49 electroplating solutions (Cupralyte 1525 and adapted Stannostar[®] SnBi). The substrate
50 was Mo-coated soda lime glass. The same substrates were also used for co-

1 electrodeposition of Cu and Bi from a solution containing 0.030 M CuSO₄, 0.010 M
2 Bi(NO₃)₃, 2 M NaOH, 0.1 M D-sorbitol. The electrolytic cell used was a standard
3 three electrode configuration. A 4 cm² substrate masked with polyimide tape was
4 connected to a rotating disc working electrode placed opposite to a large Pt foil
5 counter electrode. A saturated calomel reference electrode was used, and all potentials
6 are given vs. SCE. A μ Autolab type III potentiostat was used to carry out
7 potentiostatic plating at -0.80 V with a rotation speed of 300 rpm. The charge cut-off
8 was set as 2.1 Ccm⁻² in order to attain precursors that can be converted – after
9 complete sulfurization – into 2 μm thick films of Cu₃BiS₃ (i.e. 9 electrons per Cu₃BiS₃
10 formula unit, assuming a 100% electroplating efficiency). Films of metallic Bi were
11 vacuum-evaporated onto soda lime glass substrates, and a thickness of ~ 0.5 μm was
12 ensured by loading a calibrated amount of elemental Bi into the tungsten boat of the
13 evaporator.

14 The metal precursor samples were placed in a graphite box with an excess of
15 sulfur (0.05g) and annealed in an AS-Micro Rapid Thermal Processor (RTP)
16 (AnnealSys). The treatments were performed in the range 270 to 550 °C with dwell
17 periods in the range 5 - 960 minutes and heating rates between 5 and 600 °C·min⁻¹. A
18 static background pressure of 7·10⁴ Pa of nitrogen was maintained during annealing in
19 the RTP furnace. The dependence of the sulfur partial pressure as a function of the
20 nitrogen background pressure within our RTP system has been modelled by Scragg
21 [17]. From such modelling it can be estimated that the initial partial pressure of sulfur
22 vapour inside the graphite susceptor is ~ 5·10⁴ Pa. By consideration of the total
23 volume of the chamber and of the sulfur load, this pressure is expected to decrease to
24 ~ 2.3·10³ Pa when sulfur vapour diffusion inside the chamber is complete, with no
25 expected sulfur condensation.

26 27 28 *2.2 Film characterization*

29
30 A Panalytical X'pert X-ray powder diffractometer (XRD) was employed for structural
31 characterization of the samples. Morphological and compositional analyses were
32 performed with a Jeol 6480LV SEM connected to an INCA x-act Energy Dispersive
33 Spectroscopy (EDS) microprobe. The Cu:Bi ratios of the metallic precursors and
34 sulfurized films were estimated after acquisition of the X-Ray spectra obtained with
35 an accelerating voltage of 20kV. The M_α line of Bi and L_α line of Mo are just 0.13
36 keV apart, but the resolution of the microprobe is enough for the two contributions to
37 be discerned quite well with the software deconvolutions. Localised EDS analyses
38 averaged over several points across the films were found to be reasonably consistent
39 with those obtained by Flame Atomisation Atomic Spectroscopy (AAAnalyst 100 –
40 Perkin Elmer) on samples dissolved in concentrated HNO₃:HCl 1:1 solution (± 2% at.
41 for Bi). The EDS method was mainly employed for practical reasons. However, since
42 the energy difference between the M_α line of Mo and the K_α line of S is too small
43 (0.015 keV), it was not possible to discriminate the contributions of these two
44 elements, unless the line scan was performed in the cross section and the signals
45 compared to the micrograph (section 3.2 for details). EDS profiles of the cross
46 sections were performed on the samples previously embedded in carbon-loaded resin
47 with a Bühler moulding unit and polished up to a 0.1 μm alumina finish with a
48 universal polishing machine.

49 To assess the photoactivity of the samples, an electrolyte contact was used
50 containing 0.2 M Eu³⁺ to act as an electron (minority carrier) scavenger. A standard

1 three electrodes cell was employed to carry out the photoelectrochemical
2 characterizations with Ag/AgCl reference and a Pt wire counter electrodes, as
3 described by Scragg et al. [18]. Photovoltammograms and chronoamperometric
4 measurements were carried out under pulsed illumination provided by a white Light
5 Emitting Diode (LED), while the potential was applied and the current recorded by a
6 μ Autolab type III potentiostat.

7 External Quantum Efficiency (EQE) spectra were acquired by illuminating the
8 samples with monochromatic light of variable wavelength optically chopped at 27 Hz.
9 The photocurrent was measured with a lock-in amplifier (Stanford Research Systems).
10 The system was calibrated using a calibrated silicon photodiode traceable to National
11 Bureau of Standards standards.

14 3. Results and discussion

16 3.1 Structural characterization

17
18 The Cu/Bi/Cu precursor shows the presence of elemental Cu and Bi only, with the
19 XRD diffractogram matching the powder patterns of the elements. XRD patterns of
20 the as-deposited and annealed (without sulfur) co-electroplated (Cu_3Bi) films at 250
21 and 500 °C for 5 minutes are shown in Fig. 4.

22
23
24 The as-deposited co-electroplated (Cu_3Bi) precursor shows an XRD diffractogram
25 typical of an amorphous material; very broad peaks are seen at $\sim 18, 27, 31, 44$ and 59
26 ° (Fig. 4a), among which only those at 27 and 44 ° are centred in correspondence to
27 Bi and Cu diffractions, while the others do not match the elements' patterns. They
28 might arise from low-range ordered domains [19], whose size and quantity are such
29 that only broad and low diffraction peaks are detectable. On a larger scale the Cu and
30 Bi atoms within the film are likely to be randomly distributed.

31 Annealing at 250 °C for 5 minutes causes the elements in the co-deposit to
32 separate, forming Bi and Cu aggregates which give XRD patterns that match
33 reasonably well with the corresponding powder patterns (Fig. 4b). Annealing at 500
34 °C for 5 minutes causes the Bi and Cu aggregates to enlarge, as can be seen from the
35 sharper XRD peaks (Fig. 4c). The Bi aggregates exhibit strong (104) texturing that
36 may arise from directional crystallisation of Bi caused by the strong cooling rate
37 employed.

38 In order to relate the formation of the ternary chalcogenide to initial
39 conversion of the precursor metals into the corresponding binary sulfides, ex-situ
40 XRD analyses were performed on a series of bismuth samples sulfurized for 5
41 minutes at different temperatures between 350 and 550 °C. Films of copper were not
42 studied since it is known from previous work [16] that Cu can be fully converted to
43 CuS in the presence of elemental sulfur vapour even at temperatures as low as 200 °C,
44 with its diffraction pattern peaks being consistent with hexagonal CuS (*Covellite*).
45 The evaporated Bi samples showed a gradual greyscale variation from dark to light as
46 the temperature of the sulfurization treatment was increased. The corresponding series
47 of XRD patterns is depicted in Fig. 5.

1 The evaporated film of Bi exhibits (001) preferred orientation (Fig. 5a). This is similar
2 to what it was found for the Sb case [16]. Sulfurization for 5 minutes up to 350 °C
3 causes the Bi to react partially with sulfur, leading to a mixture of unreacted Bi and
4 Bi₂S₃. It can be observed from Fig. 5b that the remaining Bi shows a strong (012)
5 preferred orientation as opposed to (001) for the as-deposited Bi, suggesting that the
6 element has undergone melting and subsequent directional crystallisation. It is
7 interesting to note the effect possibly due to the different substrate (bare glass or Mo
8 coated glass) on the directionality of Bi crystallisation, (cf. Fig. 4).

9 The sulfurization treatments result in a bismuth sulfide with an XRD
10 diffractogram matching that of orthorhombic Bi₂S₃ (*Bismuthinite*), apart from a
11 systematic peak shift towards lower diffraction angles indicative of the presence of
12 expansion strains affecting its lattice. This strain does not seem to be appreciably
13 relieved even if the film is sulfurized up to 550 °C in the time frame of 5 minutes.
14 Since liquid Bi is denser than the solid, it is probable that Bi₂S₃ formed on the surface
15 of liquid Bi is subject to expansion strains when the substrate of unreacted Bi expands
16 during solidification. Within the 5 minutes period investigated, complete conversion
17 of Bi to Bi₂S₃ occurs at the temperature of 400 °C (Fig. 5c), when the strong peak at
18 $2\theta = 26.9^\circ$ corresponding to the (012) planes of rhombohedral Bi is no longer
19 detectable.

20 Fig. 6 shows the series of XRD patterns of the sulfurized ternary compound
21 precursors. The standard powder patterns of CuS (*Covellite*), Bi₂S₃ (*Bismuthinite*) and
22 Cu₃BiS₃ (*Wittichenite*) are also shown. The structural analysis reveals that
23 sulfurization below 400 °C leads only to the binary sulfides, leaving traces of
24 unreacted Bi. For sulfurization at 450 °C, some of the peaks related to the ternary
25 chalcogenide start to appear, but the sample still shows the coexistence of the binary
26 sulfides. At 500 °C, the conversion of the precursors to Cu₃BiS₃ is complete and the
27 treatment at 550 °C does not seem to alter appreciably the structural properties
28 attained at 500 °C.

29
30
31 The series of XRD patterns for the stacked Cu/Bi/Cu and co-electrodeposited
32 (Cu₃Bi) samples reveal very little dependence of the final phase composition of the
33 resulting film on the starting precursor configuration. Regardless of whether the
34 layered or homogenous deposits are used as precursor films, the formation of the
35 binary sulfides is observed to occur prior to the development of the ternary
36 compound.

37 In terms of phase evolution versus temperature, it is important to note that our
38 results are strikingly dissimilar to those reported by Gerein et al. [14]. In our case,
39 ternary chalcogenide was not formed at 270 °C, even with sulfurization periods
40 lasting up to 16 hours. By contrast, 5 minute treatments at temperatures above 450 °C
41 resulted in the formation of Cu₃BiS₃ films, without any loss of Bi. Indeed, no
42 appreciable Bi depletion could be detected even when the treatment at 550 °C was
43 extended to 16 hours; the resulting films were still Cu₃BiS₃ with unaltered lattice
44 parameters.

45 Gerein's sulfurization treatment consisted in the use of $\sim 7 \cdot 10^2$ Pa of hydrogen sulfide,
46 while elemental sulfur vapour was employed here, with an initial partial pressure that
47 can be estimated as $\sim 5 \cdot 10^4$ Pa at 270 °C. These different sulfurization conditions
48 might be responsible for the observed discrepancies between our work and Gerein's.

49
50

3.2 Morphological and compositional characterization

As can be seen in Fig. 7, (Cu₃Bi) precursor layers with a thickness up to 2 μm could be easily deposited, with grains of roughly the same size and a reasonably uniform Cu:Bi molar ratio distribution approaching 3:1. From the charge cut-off and the thickness of the co-deposited films, it was inferred that the co-deposited films are around 60% less dense than bulk Cu and Bi, suggesting the presence of porosity at a nanoscale level, that is not detectable with the SEM. However, the films look very uniform and therefore they were thought suitable for subsequent sulfurization treatments.

After sulfurization, the co-electroplated (Cu₃Bi) films and the Cu/Bi/Cu stacked films had the same colour. Both series of specimens were dark blue after annealing up to 450 °C, dark grey after 500 °C and light grey after 550 °C. However, the films obtained by sulfurization of (Cu₃Bi) precursors suffered from poor uniformity if the heating rate employed was higher than 5 °C min⁻¹.

The SEM analysis of the stacked Cu/Bi/Cu precursors sulfurized at 350 °C for 5 minutes with a heating rate of 600 °C min⁻¹ shows a surface comprised entirely of crystals with euhedral features identified by the EDS microprobe as CuS (Fig. 8a). The same precursor sulfurized at 500 °C for 5 minutes shows a rough surface with crystallites that appear to be poorly attached to a more compact under layer (Fig. 8b).

Invariably, for sulfurizing temperatures higher than ~270 °C and for heating rates exceeding 5 °C min⁻¹, the (Cu₃Bi) samples exhibited poor morphology and delamination (Fig. 8c). Localised EDS analysis shows the presence of Cu, Bi and S in the remaining parts of the film, while just Mo is detected on a large fraction of the sample area. On the other hand, heating rates of 5 °C min⁻¹ or less resulted in Cu₃BiS₃ films with improved adhesion and morphology (Fig. 8d-e). This can be explained by the fact that the sulfur uptake is likely to occur before the melting point of Bi is reached, when this is wholly converted to Bi₂S₃ that melts at much higher temperature (775 °C [20]). With dwell periods of 30 minutes and maximum temperature of 500 °C the film shows well-defined grains with average size of ~1 μm. The cross section micrograph (Fig. 8e) shows a film thickness of ~1.8 μm, revealing a volume expansion from the precursor of ~13%, caused by conversion to the chalcogenide. A volume expansion of ~94% is predicted based on the density difference between the bulk metals and the ternary chalcogenide. We believe that this discrepancy arises from the low density of the amorphous (Cu₃Bi) deposit employed as the precursor (which was found to be about 60% less dense than the bulk metals, Fig. 7). The compositional profile of the cross section reveals a quite even lateral distribution of the elements Cu, Bi and S; EDS localised analyses averaged over several points throughout the film show that it is slightly Cu deficient, its Cu:Bi ratio being 2.6±0.2, as for the precursor.

3.3 Photoelectrochemical characterization

The samples obtained by sulfurization of the two metal precursor configurations of at 500 °C for 30 minutes were characterised photoelectrochemically in order to ascertain

1 their minority carrier type. For this purpose, the samples were immersed in a 0.2 M
2 aqueous solution of $\text{Eu}(\text{NO}_3)_3$ and illuminated with a pulsed white LED while running
3 a cyclic voltammogram, as described in 2.2. A cathodic photocurrent response was
4 observed that corresponds to the reduction of Eu^{3+} at the surface of the working
5 electrode, showing that the samples are *p*-type.

6 Etching with a 5% wt. KCN solution improved the photoactive properties of
7 the films obtained by sulfurization of the stacked precursors. However, in contrast to
8 the behaviour seen with CuSbS_2 [16], etching periods longer than 60 seconds resulted
9 in the sudden and complete suppression of photoactivity. The samples obtained by
10 sulfurization of the (Cu_3Bi) precursors were photoactive “as-grown”, but etching with
11 a more dilute solution (0.5% wt. KCN) even for shorter periods (5 seconds)
12 suppressed their photoresponse. More work is needed in order to understand the KCN
13 etching process and its influence on surface composition and photoresponse.

14 External Quantum Efficiency (EQE) spectra of the Cu_3BiS_3 films are
15 illustrated in Fig. 9.

16
17
18 Although the photoelectrochemical properties of the films are rather poor, with
19 external quantum efficiencies below 12%, the band-gap energy of the compound can
20 be estimated as ~1.3 - 1.4 eV, which is consistent with the values reported in the
21 literature [9, 10]. It can be noticed that the onset of the EQE spectra of the samples
22 obtained by sulfurization of the (Cu_3Bi) precursor (Fig. 9a-b) is sharper than the one
23 of the $\text{Cu}/\text{Bi}/\text{Cu}$ precursor (Fig. 9c). The latter was measured after 60 seconds etching,
24 as this was required to enhance the signal. The shape of the EQE spectra of the
25 sulfurized (Cu_3Bi) films is similar, although the data corresponding to the sample
26 heated with a rate of $600\text{ }^\circ\text{C min}^{-1}$ has been multiplied by a factor of 5 for sake of
27 comparison (note the higher signal to noise ratio). This difference in the magnitude is
28 attributed to the poor morphology of the (Cu_3Bi) films sulfurized with higher heating
29 rate, as apparent from Fig.5c.

30 An order of magnitude estimate for the naturally occurring acceptor density of
31 the Cu_3BiS_3 films obtained by sulfurization of the (Cu_3Bi) precursors was obtained by
32 analysing the dependence of EQE - measured near the onset region of absorption
33 (photon energy 1.7 eV).- on applied potential. The EQE, Φ , of a semiconductor
34 photoelectrode is described by the reduced Gärtner equation as follows [18]:

35
36 (1) $\Phi = 1 - \exp(-\alpha W)$

37
38 where α is the optical absorption coefficient of the material and W is the width of the
39 space charge region. Eq. (1) is valid when the electron diffusion length, L_p , is
40 negligibly small (i.e. $\alpha L_p \ll 1$).

41 The width of the space charge region at the semiconductor-electrolyte interface is
42 given by:

43
44 (2) $W = [2\epsilon\epsilon_0(E_{FB}-E)/(eN_a)]^{1/2}$

45
46 where E is the applied potential, E_{FB} is the flat-band potential (i.e. the potential at
47 which the semiconductor energy bands are not bent), ϵ is the relative permittivity of
48 the material, ϵ_0 is the vacuum permittivity, e is the elementary charge and N_a is the
49 acceptor density for *p*-type semiconductors).

50 By combining Eqns. (1) and (2) it follows that:

$$(3) \quad [\ln(1-\Phi)]^2 = 2\alpha^2 \varepsilon\varepsilon_0(E_{FB}-E)/(eN_a)$$

Fig. 10 shows a plot of $[\ln(1-\Phi)]^2$ versus E for a typical Cu_3BiS_3 film. The linear section in the onset region has a gradient equal to $2\alpha^2 \varepsilon\varepsilon_0/(eN_a)$, from which N_a can be extracted.

Taking the value of α (at 1.7 eV) reported by Gerein et al. [10] ($\sim 6 \cdot 10^4 \text{ cm}^{-1}$), and a value of ε typical of an inorganic sulfide like CuInS_2 (10) [21], gives an acceptor density of $\sim 3 \cdot 10^{17} \text{ cm}^{-3}$. This is about one order of magnitude higher than that reported by Mesa et al. [22] for Cu_3BiS_3 films obtained by co-evaporation of the elements. It is known that typical carrier concentrations of device quality chalcogenides such as $\text{CuIn}(\text{Ga})(\text{S},\text{Se})_2$ [23] lie in the region of 10^{16} cm^{-3} , but substantially higher values are generally reported for the newer $\text{Cu}_2\text{ZnSn}(\text{S},\text{Se})_2$ absorber [24]. Further studies are required in order to estimate the electron mobility and diffusion length of the material which are key factors for its potential application in thin-film photovoltaic devices.

4. Conclusions and future work

From the series of ex-situ XRD patterns it seems that the configuration of the Bi-Cu metal precursors employed, stacked or co-deposited, does not influence the qualitative phase evolution during sulfurization. From comparison of the XRD patterns corresponding to the series of sulfurized Bi and Bi-Cu films, it appears that the formation of Bi_2S_3 is not the limiting factor for the growth of the ternary chalcogenide. The critical stage appears to be the reaction between the binary sulfides, although further studies are required to investigate this aspect.

For treatments lasting 5 minutes, the minimum temperature required for the formation of phase dominant Cu_3BiS_3 films was found to be $450 \text{ }^\circ\text{C}$. The partial pressure of $\text{S}_{2(g)}$ employed herein can be estimated as $\sim 5 \cdot 10^4 \text{ Pa}$ at $270 \text{ }^\circ\text{C}$ during the first stages of the sulfurization (slowly decreasing to a minimum of $\sim 2.3 \cdot 10^3 \text{ Pa}$ owing to $\text{S}_{2(g)}$ diffusion out of the graphite susceptor), as opposed to a pressure of only $\sim 7 \cdot 10^2 \text{ Pa}$ of H_2S employed by Gerein et al [14]. The different sulfurization conditions employed might account for the higher temperature required for the ternary chalcogenide to form in the present work. Further studies are required in order to clarify the different behaviour of the reacting atmosphere.

Reasonably homogenous and compact Cu_3BiS_3 films were obtained by sulfurization of the co-deposited (Cu_3Bi) precursors at $500 \text{ }^\circ\text{C}$ for 30 minutes provided that the heating rate was restricted to $5 \text{ }^\circ\text{C min}^{-1}$. Higher heating rates resulted in poor morphology with peeling of the film from the Mo substrate. No appreciable Bi depletion was detected in the converted compound even at $550 \text{ }^\circ\text{C}$ in the time frame up to 16 hours, the resulting films being Cu_3BiS_3 with unaltered composition and lattice parameters. It seems clear that the partial pressure of $\text{S}_{2(g)}$ employed during the treatments ($\sim 2.3 \cdot 10^3 \text{ Pa}$), is sufficient to overcome the potential Bi losses at elevated temperatures via the Le Chatelier effect on the decomposition equilibria of Cu_3BiS_3 . A detailed thermochemical investigation of such aspects would

1 be required for the definition of the temperature and $S_{2(g)}$ pressure annealing
2 boundaries. Part of these aspects are addressed in a more recent work [25].

3 The acceptor density of the deposited Cu_3BiS_3 was found to be $\sim 3 \cdot 10^{17} \text{ cm}^{-3}$
4 and the band-gap energy was estimated as $\sim 1.3 - 1.4 \text{ eV}$ with the best films showing a
5 maximum EQE of about 10% only. However, investigation of the effects of $S_{2(g)}$
6 partial pressure on the morphological and photoelectrochemical properties of the films
7 might let some room for improvement. Furthermore, if the homogeneity range of the
8 Cu_3BiS_3 phase allows some mutual solubility [9], the effect of the Cu:Bi molar ratio
9 could also be considered as a parameter for the optimisation of the film properties. In
10 this context, an approach consisting on the sulfurization of Bi-Cu 1D libraries centred
11 on the 1:3 stoichiometry would be beneficial for the rapid screening of the
12 photoelectrochemical properties.

13 The results from the present study are promising, but clearly further work
14 would be required to increase the EQE to a level where the construction of solar cells
15 becomes feasible and worthwhile.

18 Acknowledgements

19
20 We are grateful to J. M. Mitchels, A. Løken and Charles Cummings c/o University of
21 Bath for assistance with SEM analyses, preliminary work [26] and fruitful
22 discussions. The Mo coated SLG substrates were kindly provided by Stefan Schäfer
23 (Enthone). The visualizations of the crystalline structure were created with the aid of
24 VESTA software [27]. Funding was provided by the EPSRC Supergen PV-21
25 consortium.

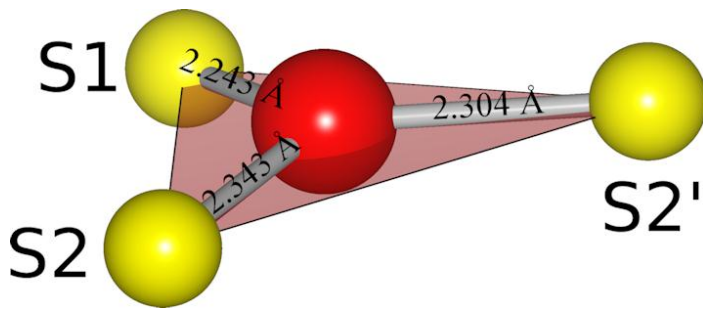
28 References

- 29
30 [1] J.F. Carlin, U.S. Geological Survey, Reston, Virginia, 2011, pp. 198.
31 [2] S. Amore, E. Ricci, G. Borzone, R. Novakovic, *Materials Science and*
32 *Engineering: A* 495 (2008) 108-112.
33 [3] B. Brunetti, D. Gozzi, M. Iervolino, V. Piacente, G. Zanicchi, N. Parodi, G.
34 Borzone, *Calphad* 30 (2006) 431-442.
35 [4] R. Novakovic, D. Giuranno, E. Ricci, S. Delsante, D. Li, G. Borzone, *Surface*
36 *Science* 605 (2011) 248-255.
37 [5] A. Sabbar, A. Zrineh, J.P. Dubès, M. Gambino, J.P. Bros, G. Borzone,
38 *Thermochimica Acta* 395 (2002) 47-58.
39 [6] P.K. Nair, L. Huang, M.T.S. Nair, H. Hu, E.A. Meyers, R.A. Zingaro, *Journal*
40 *of Materials Research* 12 (1997) 651-656.
41 [7] V. Kocman, E.W. Nuffield, *Acta Crystallographica* B29 (1973) 2528.
42 [8] E. Makovicky, *Journal of Solid State Chemistry* 49 (1983) 85-92.
43 [9] F. Mesa, A. Dussan, G. Gordillo, *physica status solidi (c)* 7 (2010) 917-920.
44 [10] N.J. Gerein, J.A. Haber, *Chemistry of Materials* 18 (2006) 6297-6302.
45 [11] V. Estrella, M.T.S. Nair, P.K. Nair, *J Semiconductor Science and Technology*
46 2 (2003) 190.
47 [12] N.J. Gerein, J.A. Haber, Photovoltaic Specialists Conference, 2005.
48 Conference Record of the Thirty-first IEEE, 2005, pp. 159-162.

- 1 [13] J.A. Haber, N.J. Gerein, T.D. Hatchard, M.Y. Versavel, Photovoltaic
2 Specialists Conference, 2005. Conference Record of the Thirty-first IEEE, 2005, pp.
3 155-158.
- 4 [14] N.J. Gerein, J.A. Haber, *Chemistry of Materials* 18 (2006) 6289-6296.
- 5 [15] A. Ennaoui, M. Lux-Steiner, A. Weber, D. Abou-Ras, I. Kötschau, H.W.
6 Schock, R. Schurr, A. Hölzing, S. Jost, R. Hock, T. Voß, J. Schulze, A. Kirbs, *Thin*
7 *Solid Films* 517 (2009) 2511-2514.
- 8 [16] D. Colombara, L.M. Peter, K.D. Rogers, J.D. Painter, S. Roncallo, *Thin Solid*
9 *Films* 519 (2011) 7438-7443.
- 10 [17] J.J. Scragg, *Copper Zinc Tin Sulfide Thin Films for Photovoltaics: Synthesis*
11 *and Characterisation by Electrochemical Methods*. Springer, 2011.
- 12 [18] J.J. Scragg, P.J. Dale, L.M. Peter, *Electrochemistry Communications* 10
13 (2008) 639-642.
- 14 [19] M. Yan, M. Scaronob, D.E. Luzzi, V. Vitek, G.J. Ackland, M. Methfessel,
15 C.O. Rodriguez, *Physical Review B* 47 (1993) 5571.
- 16 [20] D. Cubicciotti, *The Journal of Physical Chemistry* 66 (1962) 1205-1206.
- 17 [21] M. Zribi, M. Kanzari, B. Rezig, *Materials Letters* 60 (2006) 98-103.
- 18 [22] F. Mesa, G. Gordillo, T. Dittrich, K. Ellmer, R. Baier, S. Sadewasser, *Applied*
19 *Physics Letters* 96 (2010) 082113-082113-3.
- 20 [23] W.N. Shafarman, L. Stolt, in: A. Luque, S. Hegedus, (Eds.), *Cu(InGa)Se₂*
21 *Solar Cells*, John Wiley and Sons, Chichester, West Sussex PO19 8SQ, England,
22 2003.
- 23 [24] D.B. Mitzi, O. Gunawan, T.K. Todorov, K. Wang, S. Guha, *Solar Energy*
24 *Materials and Solar Cells* 95 (2011) 1421-1436.
- 25 [25] D. Colombara, L.M. Peter, K.D. Rogers, K. Hutchings, *Journal of Solid State*
26 *Chemistry* 186 (2012) 36-46.
- 27 [26] P.J. Dale, L.M. Peter, A. Loken, J. Scragg, *ECS Transactions* 19 (2009) 179-
28 187.
- 29 [27] K. Momma, F. Izumi, *Journal of Applied Crystallography* 41 (2008) 653-658.
- 30
31

1 **List of figures and captions**

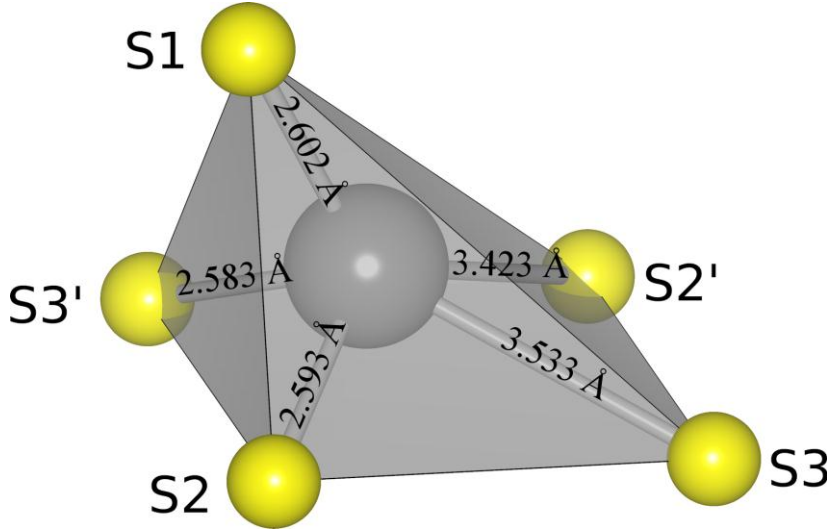
2
3



4
5

6 **Fig 1** (Colour online) Trigonal planar CuS₃ unit showing the coordination of Cu
7 atoms in the structure of Cu₃BiS₃ and the distances between Cu (red) and S (yellow)
8 atoms.
9

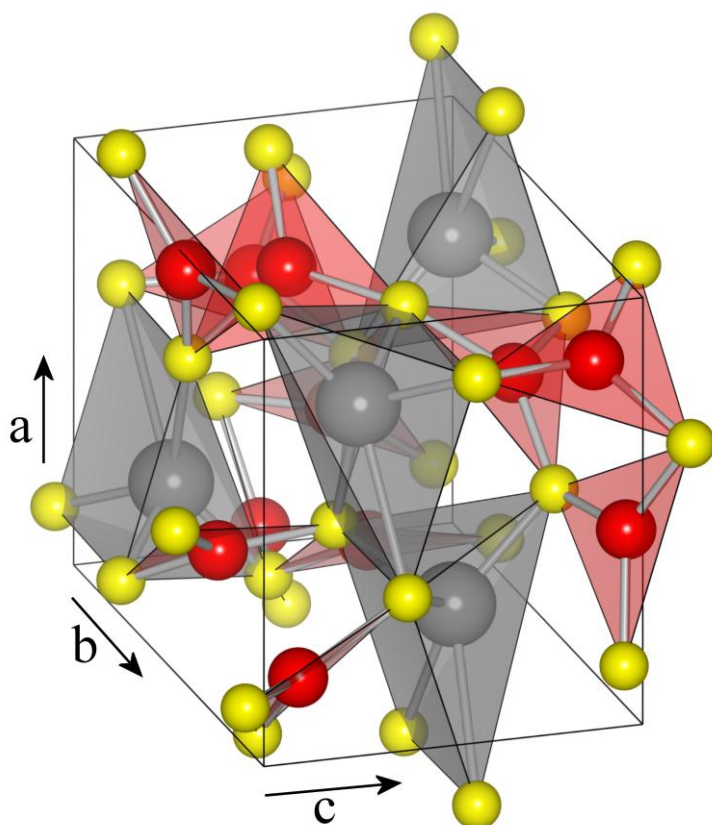
10



11
12

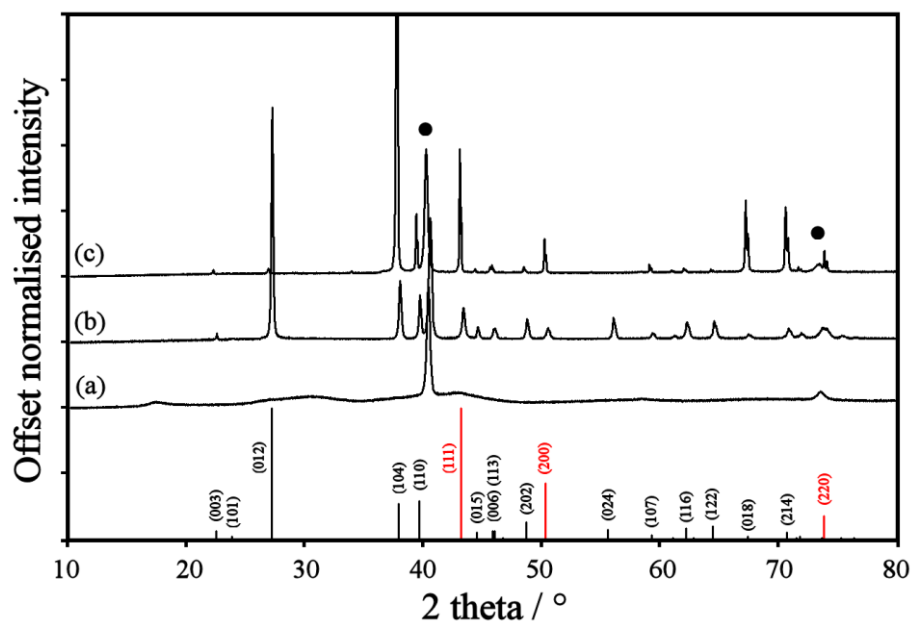
13 **Fig 2** (Colour online) Distorted square pyramidal BiS₅ unit showing the coordination
14 of Bi atoms in the structure of Cu₃BiS₃ and the distances between Bi (grey) and S
15 (yellow) atoms.
16

17



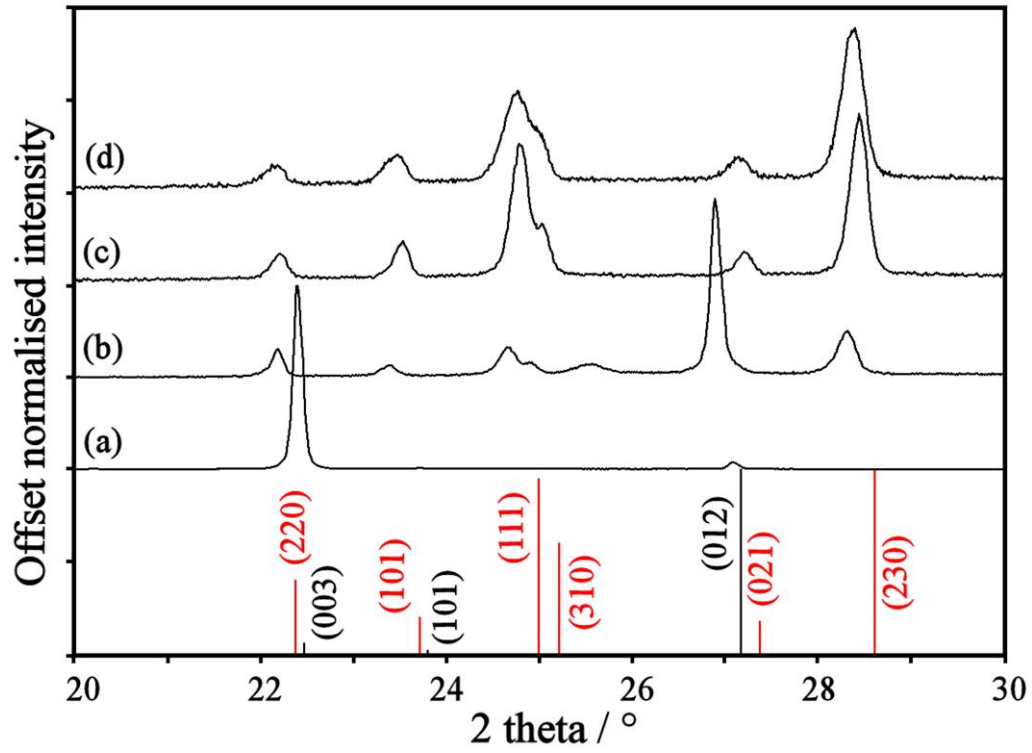
1
2
3
4
5
6

Fig 3 (Colour online) Unit cell of Cu_3BiS_3 showing trigonal planar CuS_3 (red) and distorted square pyramidal BiS_5 units (grey) and S atoms (yellow).



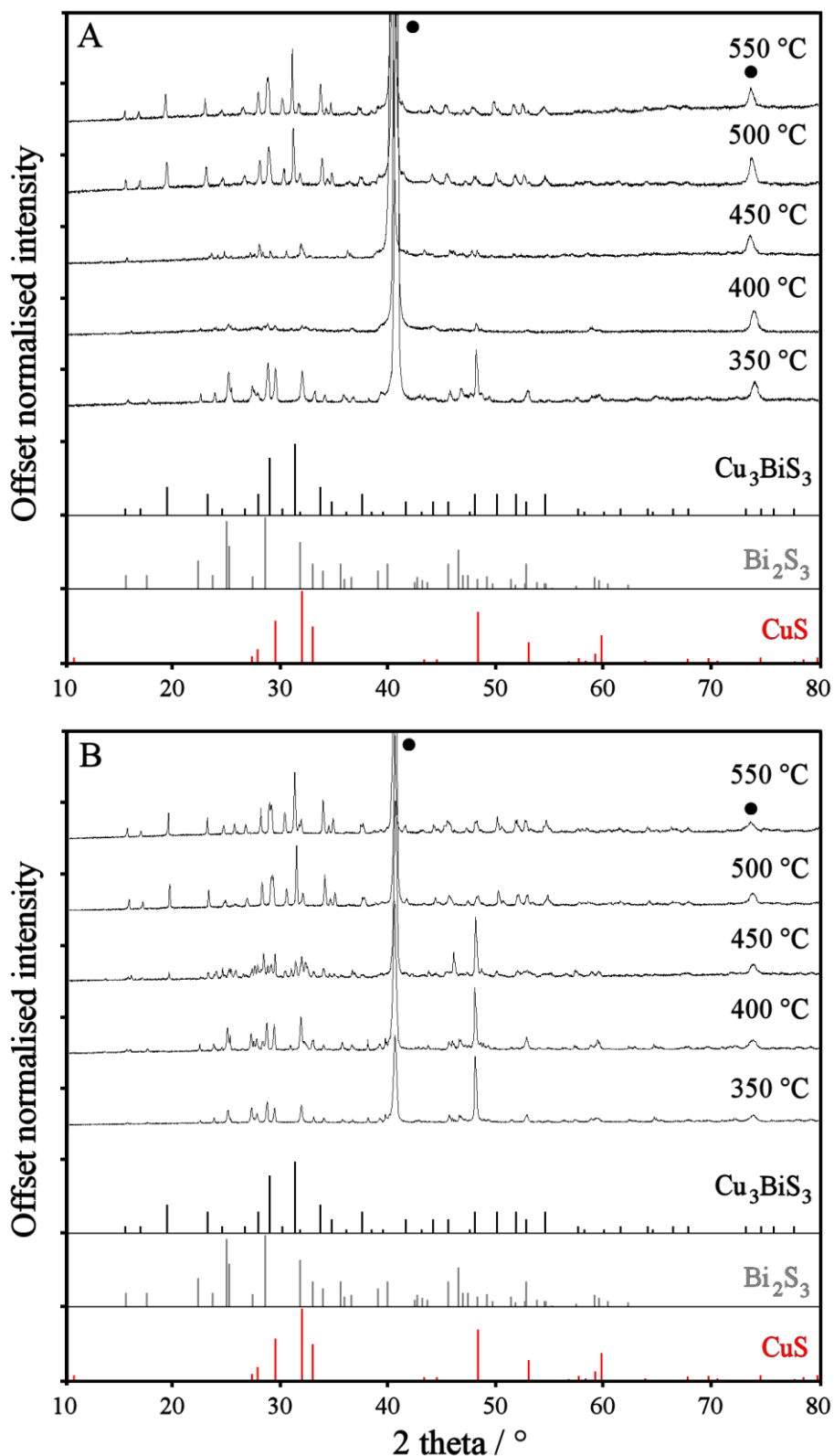
7
8
9
10
11
12

Fig 4 XRD patterns of the Cu_3Bi electroplated precursors as-deposited (a) and after thermal treatment at 250 (b) and 500 °C (c) for 5 minutes. Standard powder patterns for Bi PDF no 44-1246 (black) and Cu PDF no 70-3038 (red) are included (● labels refer to the Mo substrate).



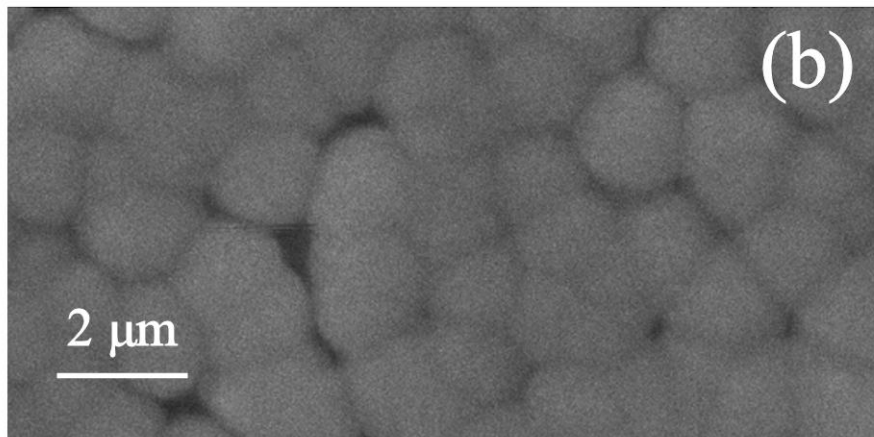
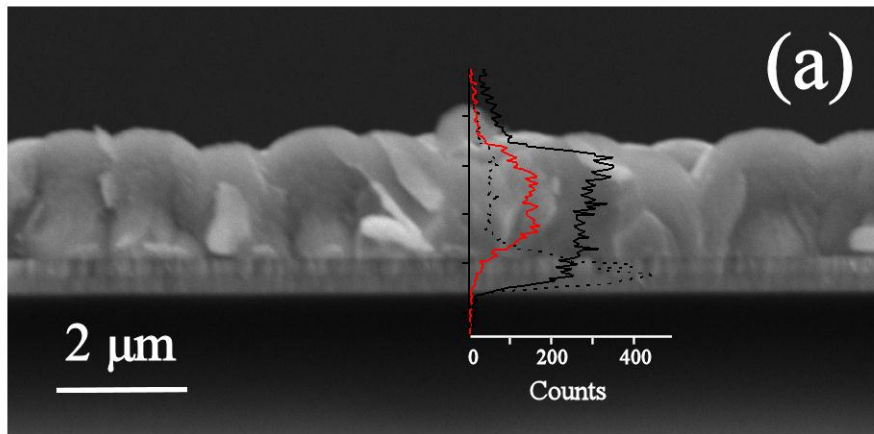
1
2
3
4
5
6
7
8

Fig. 5 Series of XRD patterns of the evaporated Bi films as deposited (a) and after sulfurization at 350 (b), 400 (c) and 450 °C (d) for 5 minutes with fast heating rate (600 °C·min⁻¹). Standard powder patterns for Bi PDF no 44-1246 (black) and Bi₂S₃ PDF no 6-333 (red) are included. The substrate employed is soda-lime glass.



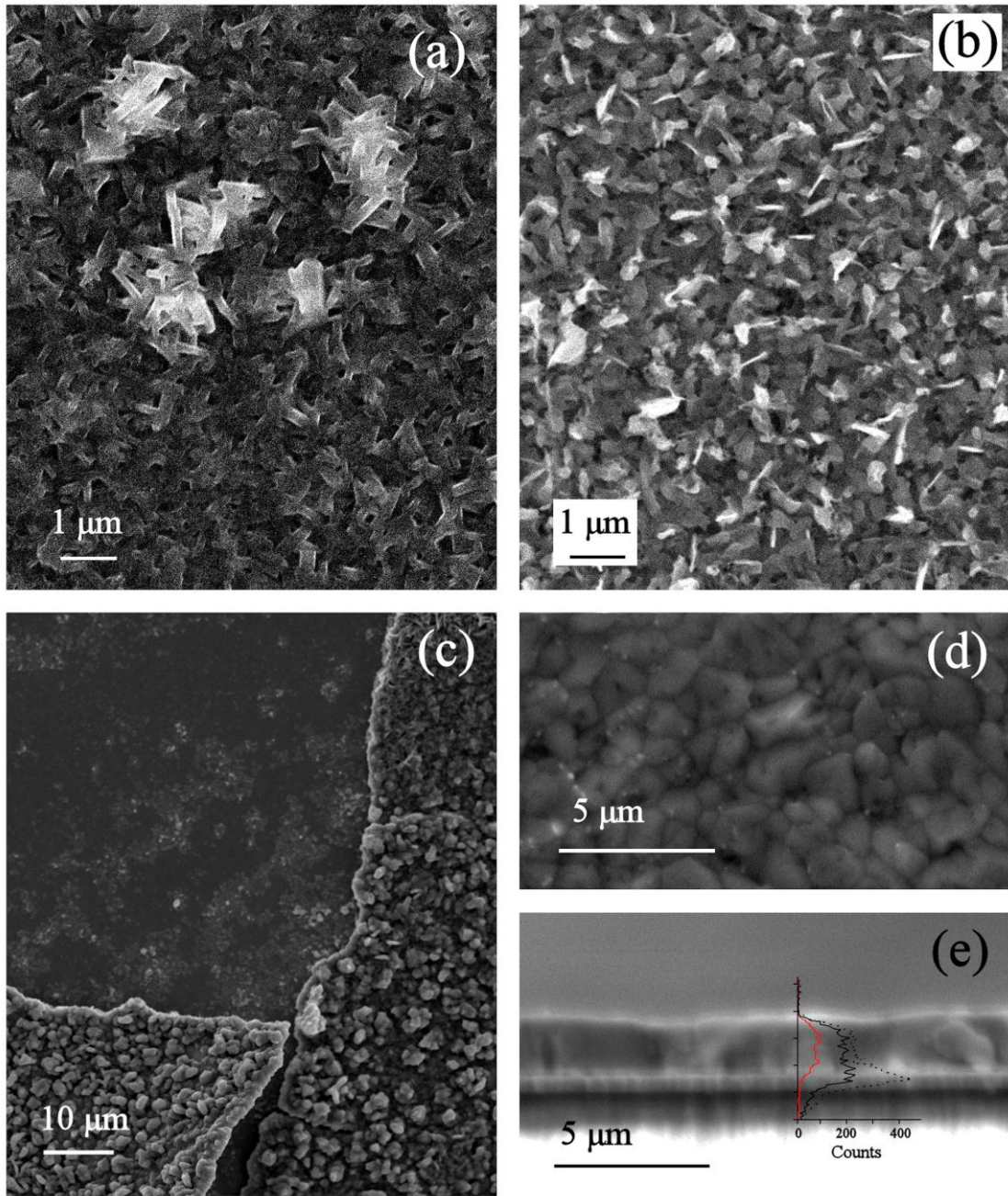
1
2
3
4
5
6
7

Fig. 6 Series of XRD patterns of typical Cu/Bi/Cu stacked (A) and Cu_3Bi (B) precursors after sulfurization at temperatures between 350 and 550 °C for 5 minutes (heating rate: 600 °C·min⁻¹). Standard powder patterns of the relevant phases: CuS PDF no 65-3561 (red), Bi_2S_3 PDF no 6-333 (grey) and Cu_3BiS_3 PDF no 9-488 (black) (● labels refer to the Mo substrate).



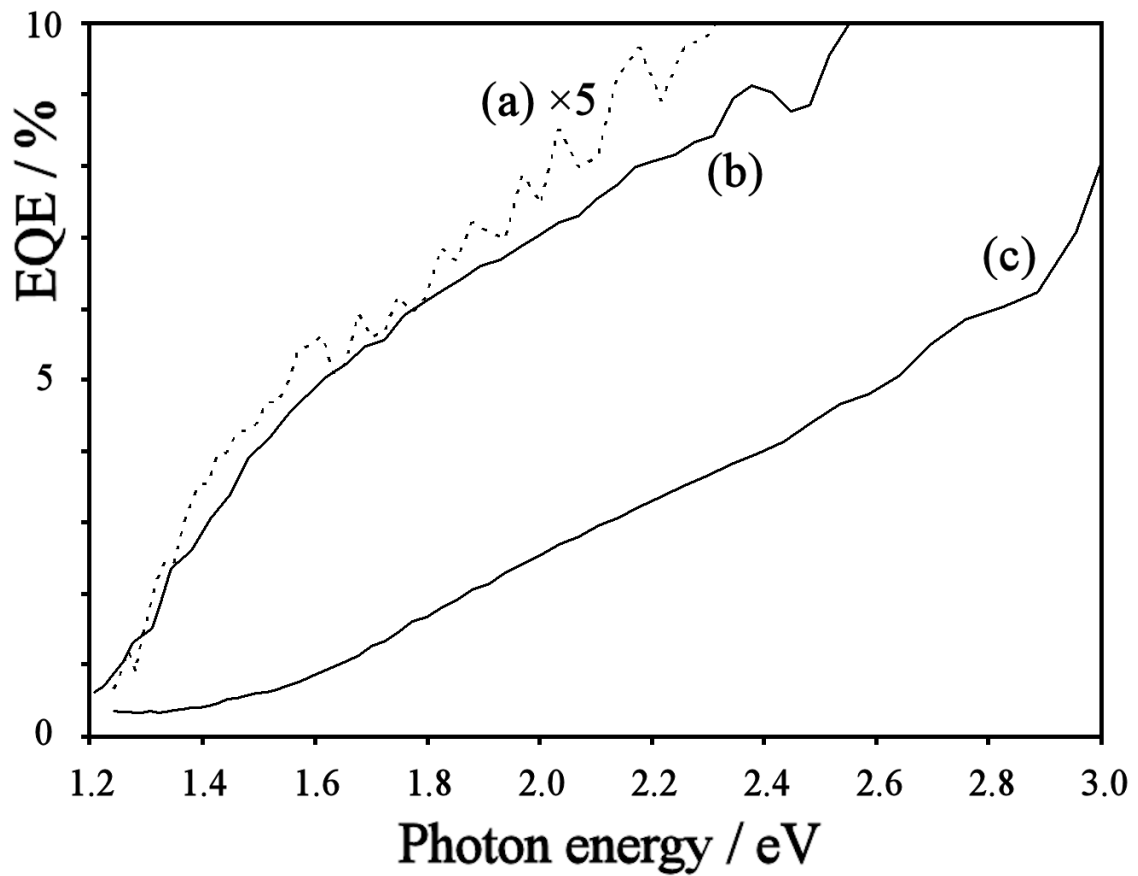
1
2
3
4
5
6
7

Fig. 7 SEM cross section (a) and top view (b) of an as deposited (Cu_3Bi) precursor. The inset shows the EDS compositional profile corresponding to Cu (red), Bi (black) and Mo (dashed), performed on the same sample embedded in carbon loaded resin.



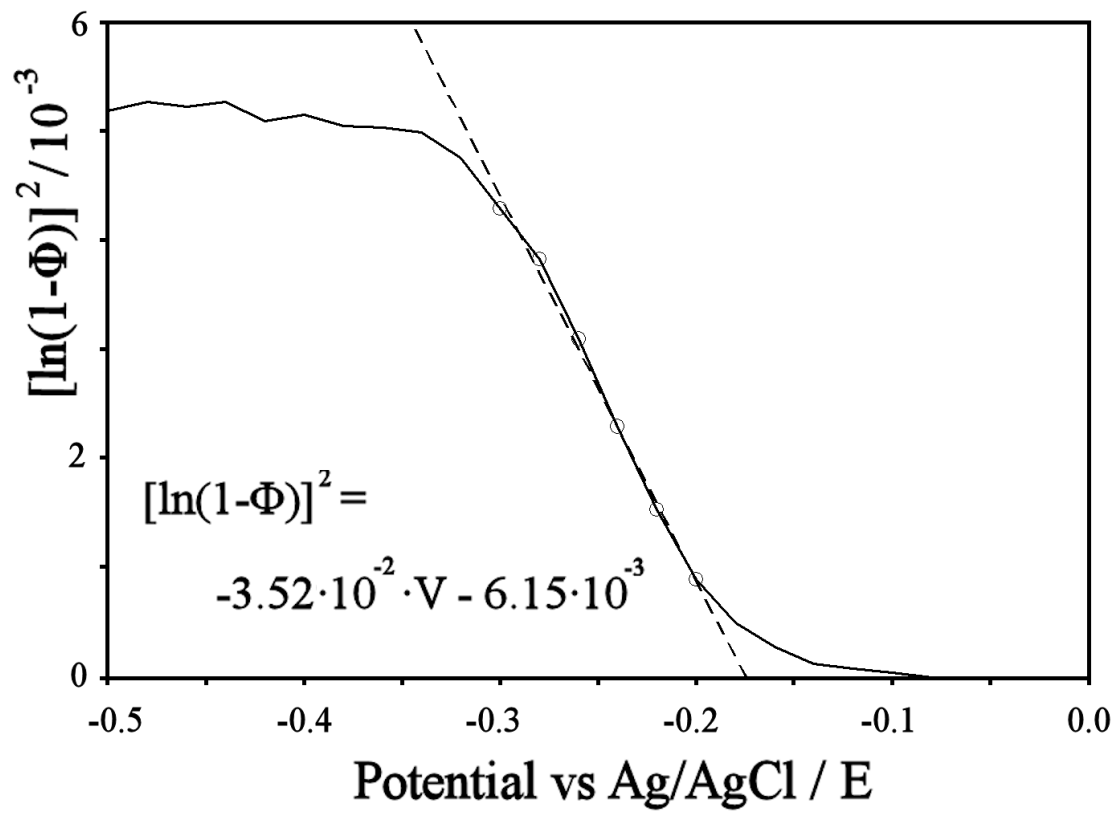
1
2
3
4
5
6
7
8

Fig. 8 SEM top views of typical Cu/Bi/Cu stacked precursor sulfurized at 350 °C (a) and 500 °C (b) for 5 minutes with heating rate of 600 °C min⁻¹. Morphology of (Cu₃Bi) precursors after sulfurization at 350 °C for 5 minutes with heating rate of 600 °C min⁻¹ (c) and at 500 °C for 30 minutes at 5 °C min⁻¹ (d, e). Inset (e): EDS compositional profile corresponding to Cu (red), Bi (black), Mo and S (dashed).



1
2
3
4
5
6
7
8

Fig. 9 EQE spectra of Cu_3BiS_3 films obtained by sulfurization of the Bi-Cu metal precursors at $500\text{ }^\circ\text{C}$ for 30 minutes. Cu_3Bi precursor with heating rate of $600\text{ }^\circ\text{C min}^{-1}$ (x5) (a) and $5\text{ }^\circ\text{C min}^{-1}$ (b); Cu/Bi/Cu precursor with 60 seconds etching in KCN 5% wt. (c). Acquisition conditions: 0.2 M Eu^{3+} solution, -0.5 V vs. Ag/AgCl, chopping frequency 27 Hz .



1
2
3
4
5

Fig. 10 Plot of $[\ln(1-\Phi)]^2$ vs applied potential of a typical Cu_3BiS_3 film obtained by sulfurization of a Cu_3Bi precursor at 500 °C for 30 minutes. Acquisition conditions: 0.2 M Eu^{3+} solution, 1.7 eV, chopping frequency 27 Hz.